



OPEN

Clinical and brain functional correlates of instrumental rigidity measurement in Parkinson's disease

Yoshikazu Nakano^{1,2}, Shigeki Hirano^{1✉}, Mitsuyoshi Tamura¹, Yume Koizumi¹, Yoshihisa Kitayama¹, Michiko Izumi¹, Masahide Suzuki¹, Kosuke Yamagishi¹, Yutaro Suzuki¹, Shinobu Ikeda³, Ayaka Arase³, Tatsuya Yamamoto^{1,4}, Yoshitaka Yamanaka^{1,5,6}, Atsuhiko Sugiyama¹, Kazumoto Shibuya¹, Takuro Horikoshi⁷, Takashi Uno⁷, David Eidelberg² & Satoshi Kuwabara¹

Rigidity, a cardinal symptom of Parkinson's disease (PD), remains challenging to assess objectively. A torque-angle instrument was developed to quantify muscle tone, providing two parameters: bias difference and elastic coefficient. This study aimed to investigate the association of the instrument-measured rigidity with clinical assessments and brain function. In 30 patients with PD, the muscle tone in both arms was evaluated. Ten with wearing-off phenomenon were assessed twice, off and on condition. Twenty-nine patients underwent brain perfusion single-photon emission computed tomography (SPECT), and expression of PD-related covariance pattern (PDRP) was computed. Bias difference and elastic coefficient showed positive correlations with physician-rated rigidity ($P < 0.002$). Bias difference decreased after dopaminergic medication ($P = 0.022$) and was associated with lower body mass index ($P = 0.012$). Elastic coefficient positively correlated with the Unified PD Rating Scale Part III and PDRP scores ($P < 0.044$). Furthermore, the higher bias difference correlated with decreased sensory-motor cortex and increased substantia nigra perfusion ($P < 0.001$). The Torque-angle instrument is a viable tool for quantifying rigidity in PD. The bias difference reflects treatment responsiveness and is associated with the function in the sensory-motor cortex and substantia nigra. The elastic coefficient is indicative of overall Parkinsonism severity.

Keywords Parkinson's disease, Rigidity, Torque-angle measurement, Brain perfusion, Single photon emission tomography (SPECT), Network analysis

While the pandemic of COVID-19 had significantly hampered conventional means for patients to receive medical care, telemedicine became more popularized. This innovation has led healthcare providers to assess motor symptoms without physical contact with patients¹. Recent technological advances, including motion capture and artificial intelligence, have further streamlined the automated assessment of motor symptoms². For individuals suffering from movement disorders such as Parkinson's disease (PD), the burden of hospital visits may be alleviated by the benefits of video-based technologies^{1,3}. However, muscle tone, including rigidity, a cardinal feature of Parkinsonism, cannot be assessed without manual physical examination by a physician, which remains a limitation in video-based motor evaluation⁴.

A Japanese research group introduced an instrument employing two force sensors and a gyroscope to quantify muscle tone⁵. It depicts torque-angle graphs during passive extension and flexion of the elbow joint (Supplemental video), providing two parameters: the elastic coefficient and the bias difference (termed as the “sum of the difference of bias” in the original article). They showed that these parameters correlated positively

¹Department of Neurology, Chiba University Graduate School of Medicine, 1-8-1, Inohana, Chuo-ku, Chiba 264-8670, Chiba, Japan. ²Center for Neurosciences, The Feinstein Institutes for Medical Research, Manhasset, NY, USA. ³Division of Laboratory Medicine, Chiba University Hospital, Chiba, Chiba, Japan. ⁴Division of Occupational Therapy, Department of Rehabilitation, Chiba Prefectural University of Health Sciences, Chiba, Chiba, Japan. ⁵Urayasu Rehabilitation Education Center, Chiba University Hospital, Urayasu, Chiba, Japan. ⁶Department of Rehabilitation, Kimitsu Chuo Hospital, Kimitsu, Chiba, Japan. ⁷Diagnostic Radiology and Radiation Oncology, Chiba University Graduate School of Medicine, Chiba, Chiba, Japan. ✉email: s_hirano@chiba-u.jp

with the physician-rated rigidity score of the Unified PD Rating Scale (UPDRS) motor subscore (part III) in patients with PD. However, the difference between the two parameters remains elusive, and the correlation between these parameters and clinical biomarkers remains unexplored.

The landscape of PD research has witnessed the establishment of diverse clinical biomarkers over the past decades, serving purposes ranging from differential diagnosis to disease tracking⁶. Among diverse clinical biomarkers, the Parkinson's disease-related covariance pattern (PDRP) has emerged as a robust imaging biomarker, derived initially from brain network analysis with ¹⁸F-fluorodeoxyglucose positron emission tomography (FDG PET) and subsequently applied to other kinds of resting-state brain images including perfusion single-photon emission computed tomography (SPECT)^{7–10}. PDRP stands validated globally for its efficacy in differential diagnosis and disease monitoring^{11,12}.

The present study aimed to validate the muscle tone-measuring instrument in patients with PD and elucidate the relationships between the rigidity measured by the instrument and pertinent clinical features, including PDRP derived from perfusion SPECT images.

Methods

Subjects and clinical assessment

Thirty patients with PD (13 women and 17 men, age 66.8 ± 7.2 years old (mean \pm standard deviation)) were recruited between June 2017 and September 2019 at the Department of Neurology, Chiba University Hospital. They fulfilled the established criteria of the Movement Disorders Society¹³. Five patients were drug-naïve. Of the remaining 25 patients, three were on levodopa monotherapy, and the other 22 patients were on other dopaminergic medications, such as dopamine agonists and/or monoamine-B inhibitors. Of these 22 patients, nine had deep brain stimulation (DBS) on bilateral subthalamic nuclei (Supplementary Table 1). None of the participating patients showed dyskinesia. Rigidity was quantified with the torque-angle instrument in half of the 30 patients under medication and in the other half under off conditions. The OFF-medication condition was defined as more than twelve hours of discontinuation of dopaminergic medication. Patients with DBS were tested under ON medication and ON stimulation. Ten out of patients tested in the off condition, who had wearing-off, were retested after dopaminergic medication. Two different examiners conducted tests on a single arm to ensure reliability, and the results were averaged for analysis. Concurrently, physician-rated rigidity scores based on the UPDRS ranging from 0 to 4 (0 = absent; 1 = slight; 2 = mild to moderate; 3 = marked; 4 = severe) were evaluated by a movement disorder specialist blind to the instrument-measured values¹⁴. The total UPDRS part III score was assessed in off condition. Clinical information such as disease duration, body mass index, L-dopa equivalent daily dose, and Mini-Mental State Examination scores were collected^{15,16}. This study was approved by the Observational Research Ethics Review Committee at the Chiba University Hospital (#2052 and #3073), and written informed consent was obtained from all participating patients. Furthermore, all methods were performed in accordance with the ethical principles outlined in the Declaration of Helsinki.

Muscle tonus measurement instrument

Rigidity was quantified utilizing the Muscle Master (MTM-05), developed by Medicalnics Co., Ltd., Japan (<http://www.medicalnics.co.jp/en/posts/product1.html>). Prior to the measurement, the patient's arm length and body weight were measured to calculate torque. This instrument incorporates a sensor unit comprising two three-axis force sensors and a gyroscope. During the measurement, the examiner positioned the patient's wrist between two force sensors, maintaining a horizontal orientation, while the patient reclined in a supine position on the bed and was instructed to remain relaxed. The examiner systematically flexed and extended the patient's elbow, with each movement lasting 1.0 s and intervals of 4.5 s at the extended and flexed positions (Supplemental video). The Muscle Master dynamically captured torque at various elbow joint angles (see Fig. 1). The regression line was derived from torque changes observed during five cycles of elbow flexion and extension within the calculation range of 10 to 110 degrees. The slope of this line was designated as the elastic coefficient. The original methodology involved calculating elastic coefficients separately for flexion and extension⁵. However, torque-angle lines showed consistent parallels between the two movements in nearly all measurements, exhibiting a close correlation (as shown in Supplementary Fig. 1). Consequently, these values were averaged and treated as a single parameter. Another rigidity parameter, bias difference, was defined as the cumulative torque difference between flexion and extension at 30, 60, and 90 degrees. To ensure reliability, two different examiners conducted tests on a single arm, and the results were averaged for analysis.

Imaging acquisition and preprocessing

Twenty-nine out of the 30 patients underwent cerebral blood flow SPECT in the OFF condition, more than twelve hours without dopaminergic medications. Patients with DBS were scanned under OFF medication and ON stimulation. The interval between muscle tone measurement and SPECT scan was 4.8 ± 2.3 months (mean \pm S.D.). Following a five-minute post-injection period of 111 MBq N-isopropyl-p-¹²³I-iodoamphetamine (¹²³I-IMP), the GE Infinia Hawkeye 4 system (General Electric Company, USA) conducted whole-brain scans for 24 min. The scans utilized 4.42 mm thick slices of a 64*64 matrix, employing 8 rotations lasting 3 min each, with four-degree steps. Subsequently, these images underwent reconstruction utilizing a Butterworth filter with a cutoff frequency of 0.5 cycle/cm and 8 orders. Additionally, Chang's attenuation correction with a coefficient of 0.07 was applied.

After conversion from DICOM to NIfTI format using dcm2nii in MRICroGL (<https://www.nitrc.org/projects/mricrogl>), the normalization onto the Montreal Neurological Institute (MNI) space and smoothing with Gaussian filter of full width at half maximum at 14 mm was applied using SPM 8 (<https://www.fil.ion.ucl.ac.uk/spm/software/spm8/>), running on MATLAB 2020a (MathWorks, Inc, USA). Regional cerebral blood flow was determined by a voxel-wise ratio to the respective whole-brain mean. For the network analysis, as detailed in

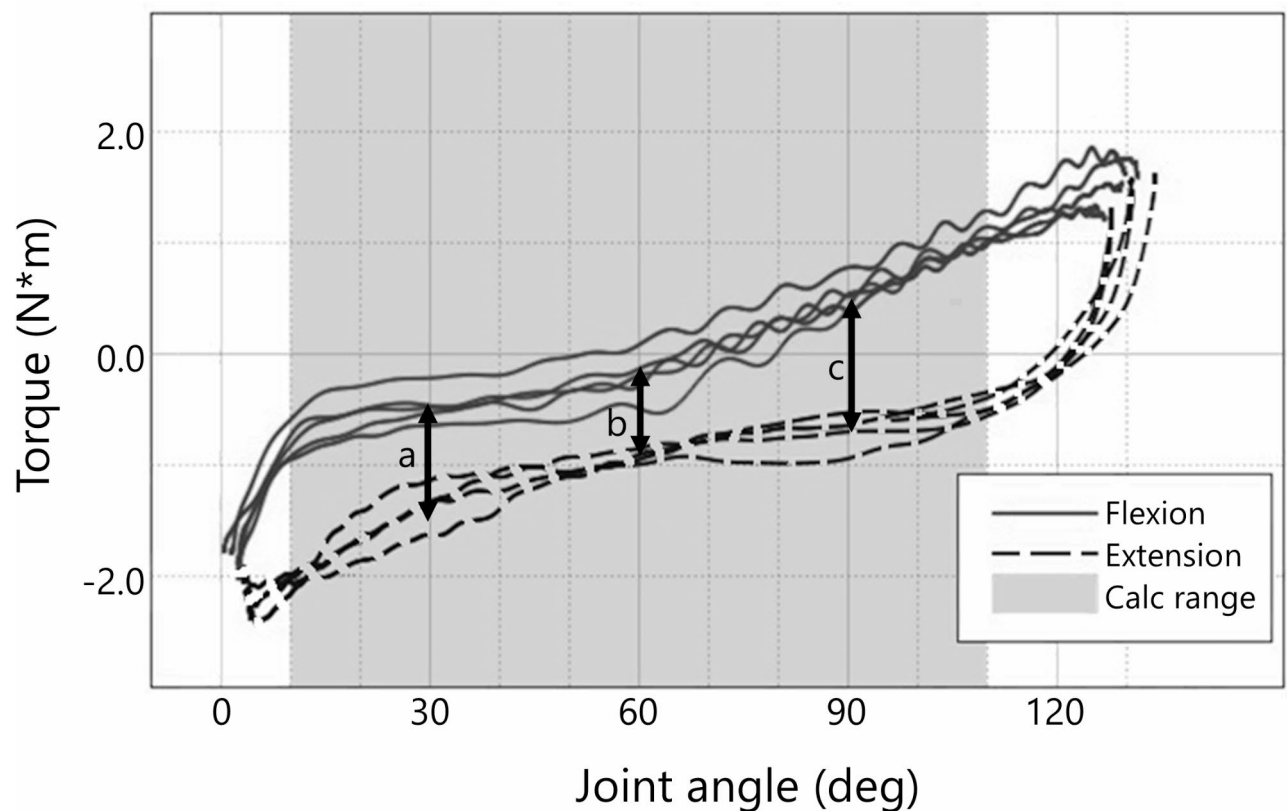


Fig. 1. The torque-angle graph on the muscle tonus measuring instrument depicts the dynamic relationship between torque and elbow angle during passive flexion (solid line) and extension (dashed line). The bias difference is defined as the sum of the discrepancies (indicated by double arrows) between flexion and extension torques at 30, 60, and 90 degrees ($a + b + c$). The elastic coefficient is calculated as the estimated slope of the regression.

the subsequent section, images were converted from NIfTI to ANALYZE format using ScAnVP version 7.1 (<https://feinsteinneuroscience.org/imaging-software/download-software>) and subsequently resliced to the same dimension as the default PET mask image included in ScAnVP¹⁷.

PD-related perfusion pattern identification

To delineate the SPECT-derived PD-related perfusion pattern (PDRP), we utilized a dataset comprising 17 healthy controls (8 men and 9 women, age 66.7 ± 9.9 years (mean \pm S.D.)) and age- and sex-matched 17 PD patients (10 men and 7 women, age 65.0 ± 9.6 years (mean \pm S.D.)), who underwent perfusion SPECT with ^{123}I -IMP in off-medication state (Supplementary Table 2). Healthy controls were volunteers without a history of psychiatric or neurological symptoms. The PD patients were diagnosed using the Movement Disorders Society criteria¹³, and none of them had deep brain stimulation therapy. There was no overlap between the PD patients in this pattern identification cohort and those in the rigidity test cohort. The network analysis using scaled subprofile modeling of principal component analysis was executed on ScAnVP on the dataset of 34 scans, and each subject's PDRP score was calculated as previously reported¹⁷.

Rigidity parameters and regional blood flow (separated by left and right)

On 60 results obtained from both arms of 30 patients, Spearman's rank correlation tests were performed for corresponding physician-rated rigidity score, bias difference, and elastic coefficient. These values were then compared between the off and on conditions in the 10 PD subgroup using a paired t-test.

To identify the brain region associated with physician-rated rigidity and instrumental measurement, a voxel-wise multiple regression was performed in SPM8. The objective variables consisted of perfusion images, while the bias difference or the elastic coefficient of the right or left arm was used separately as the explanatory variable. Age, sex, and medication condition on the rigidity test were incorporated as covariates, and a threshold mask with a relative 0.8 and an implicit mask were applied for the analysis. Additionally, a unilateral brain mask was used as an explicit mask to focus on the contralateral cerebrum and midbrain and the ipsilateral cerebellum, pons, and medulla on the side of the explanatory variables. Clusters with more than 30 voxels and an uncorrected p-value below 0.001 were considered significant.

Clinical data and PDRP related to subjects' rigidity scores (left-right averaged)

To explore associations with clinical characteristics and PDRP expression score, correlation analyses were performed for the left-right-averaged bias difference and elastic coefficient in each patient. The Anderson-Darling test was used to assess the normality of variables. Pearson's correlation test was applied to normally distributed variables (Anderson-Darling $P > 0.05$), while Spearman's rank correlation test was used for non-normally distributed variables (Anderson-Darling $P < 0.05$). After P values were adjusted by Bonferroni correction, significance was considered at a threshold below 0.05.

Results

The two instrumental rigidity parameters, the bias difference, and elastic coefficient, correlated with the physician-rated rigidity score in PD ($\rho = 0.64$ and $\rho = 0.40$, $P < 0.004$, Fig. 2AB). These two muscle tone parameters did not correlate with each other ($\rho = 0.23$, $P = 0.076$, Fig. 2C). By administration of PD medication, the intra-individual assessment showed a reduction in the physician rigidity scale ($P = 0.047$) and the bias difference ($P = 0.022$) but not the elastic coefficient ($P = 0.096$) (Fig. 2D–F).

The principal component analysis showed the first and third principal components effectively discriminated between healthy controls and PD ($P < 0.05$). Their linear combination explained 22.6% of the total variance and was defined as PDRP because it had a lower Akaike information criterion than either component alone (PC1 = 24.6, PC3 = 46.3, and PC1&3 = 24.4). The PDRP topography showed bilateral cerebellum, pons, and right sensorimotor cortex hyperperfusion and bilateral posterior parietal cortex, premotor cortex, middle cingulate cortex, and thalamus hypoperfusion (Fig. 3A). Applying this covariance pattern to each PD patients undergoing rigidity testing with the device yielded individual PDRP scores. This subject expression score of the PDRP score showed a positive correlation with the elastic coefficient ($r = 0.42$, $P = 0.044$, Fig. 3B) but not with the bias difference ($r = -0.04$, $P = 1.00$, Fig. 3C).

For the left-right averaged value for each patient and clinical features, the bias difference correlated negatively with the body mass index ($r = -0.49$, $P = 0.012$), the elastic coefficient correlated positively with UPDRS part III ($r = 0.45$, $P = 0.026$) (Table 1).

Voxel-wise brain analysis revealed the left physician-rated rigidity correlated positively with perfusion in the right midbrain including substantia nigra and red nucleus and negatively with right sensory-motor cortex perfusion (Fig. 4A). The right physician-rated rigidity correlated negatively with left sensory-motor cortex perfusion (Fig. 4B). The left bias difference correlated positively with the perfusion in the right substantia nigra and negatively with the right sensory-motor cortex perfusion (Fig. 4C). The right bias difference correlated

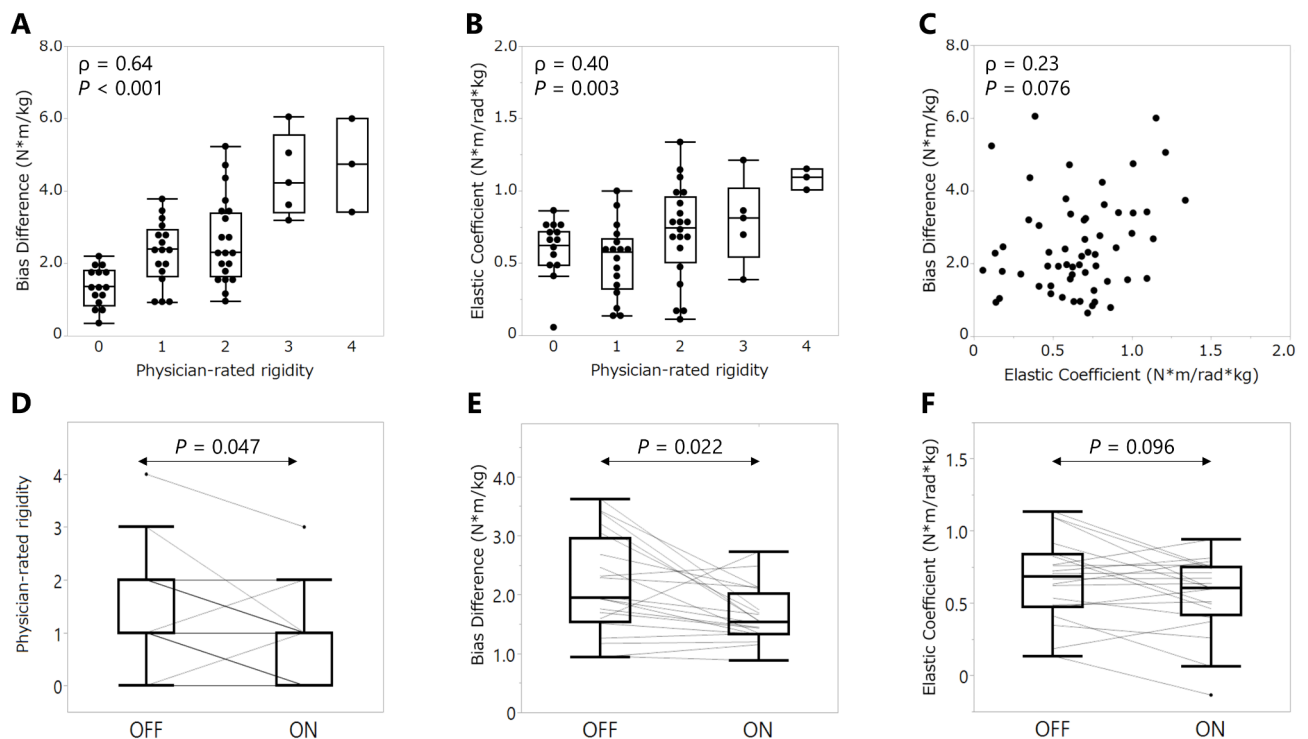
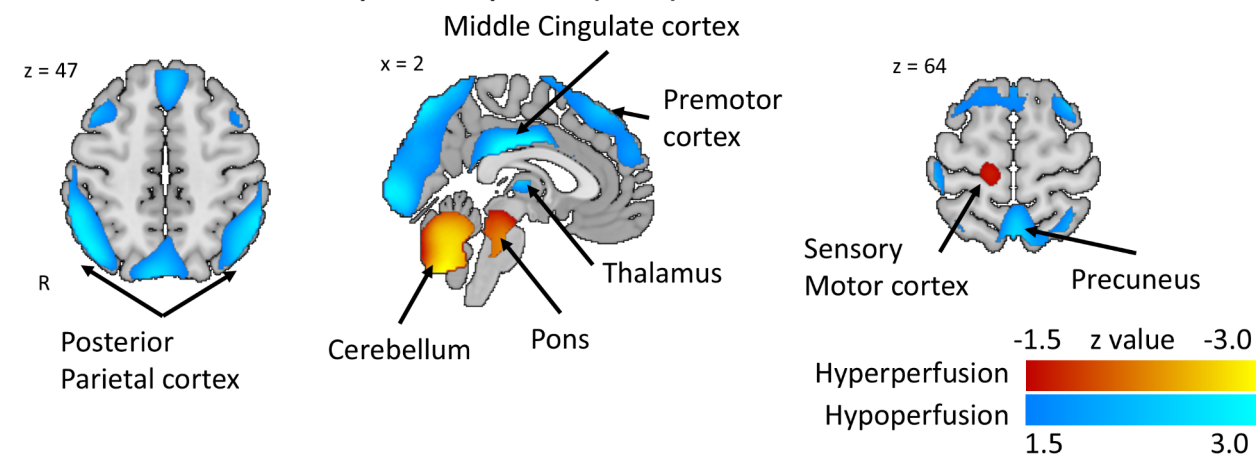
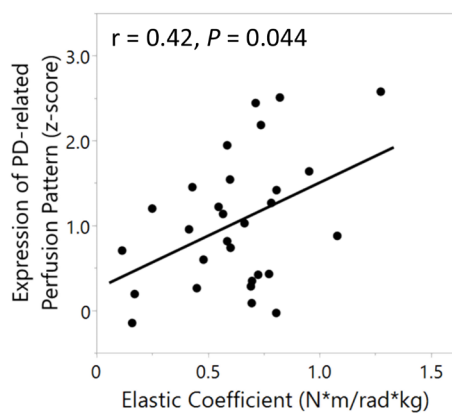


Fig. 2. (A–C) Instrumental rigidity parameters, bias difference, and elastic coefficient were correlated with physician-rated rigidity score. Spearman's correlation coefficient (ρ) and P-values after Bonferroni correction are shown. (D–F) In ten patients with wearing-off, physician-rated rigidity score and bias difference were diminished by dopaminergic medication, though the elastic coefficient remained stable. P values refer to paired t-test and Bonferroni correction.

A. Parkinson’s disease-related perfusion pattern (PDRP)



B. Elastic Coefficient and PDRP



C. Bias difference and PDRP

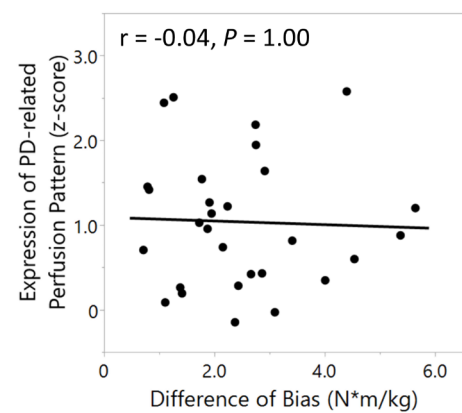
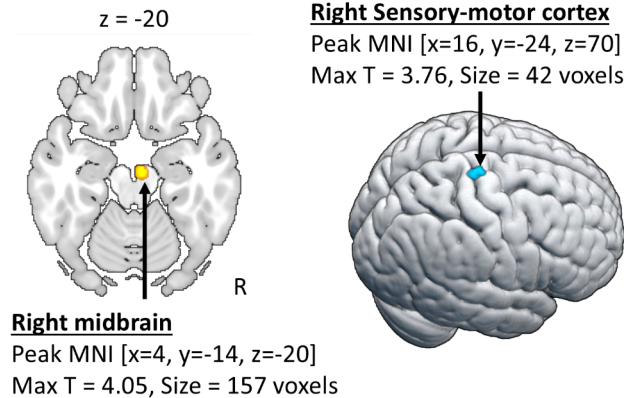


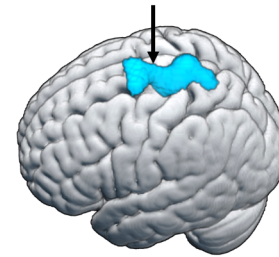
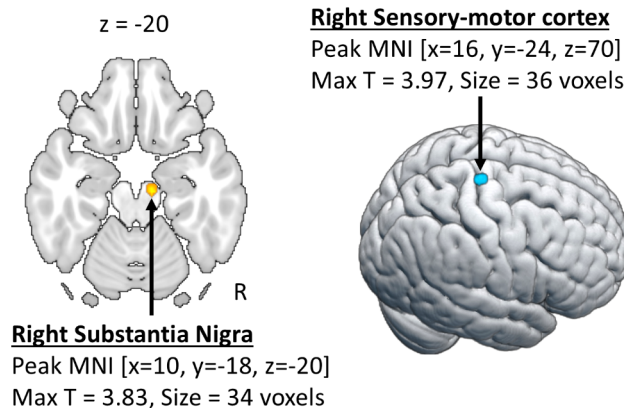
Fig. 3. (A) The Parkinson’s disease (PD)-related covariance pattern (PDRP) was identified with cerebral blood flow SPECT in PD pattern identification cohort and healthy controls. It shows hyperperfusion in the bilateral cerebellum, pons, and right sensorimotor cortex (red-yellow) and hypoperfusion in the bilateral posterior parietal cortex, premotor cortex, middle cingulate cortex, and thalamus (blue-cyan), presented on T1-weighted magnetic resonance image templates. (B,C) The elastic coefficient correlated with PDRP expression, but the bias difference did not.

Clinical data	Mean ± S.D.	Bias difference		Elastic Coefficient	
		Coefficient	P value	Coefficient	P value
Age (year)	66.8 ± 7.2	0.075	1.00	− 0.023	1.00
Disease duration (year)	6.40 ± 3.77	− 0.22	0.49	− 0.083	1.00
Body mass index (kg/m²)	23.2 ± 4.9	− 0.49	0.012	0.21	0.51
Arm length (cm)	23.7 ± 1.4	− 0.11	1.00	− 0.22	0.47
L-dopa equivalent daily dose (mg)	720 ± 404	− 0.080	1.00	0.11	1.00
UPDRS III	37.8 ± 17.5	0.27	0.28	0.45	0.026
Mini-mental state exam	28.3 ± 1.8	− 0.18	0.72	− 0.19	0.71

Table 1. Clinical correlation of instrument-measured rigidity. Spearman’s rank correlation coefficients are shown for age and Mini-Mental State Exam, which were not normal distribution (Anderson-Darling test’s P value = 0.014, and < 0.001, respectively). Other coefficients are Pearson’s correlation. P values are corrected by Bonferroni method. S.D.: Standard deviation.

A. Left Physician-rated rigidity**B. Right Physician-rated rigidity**

Left Sensory-motor cortex
Peak MNI [x=-18, y=-6, z=72]
Max T = 4.37, Size = 1348 voxels

**C. Left Bias Difference****D. Right Bias Difference**

Left Sensory-motor cortex
Peak MNI [x=-12, y=-34, z=72]
Max T = 4.05, Size = 181 voxels

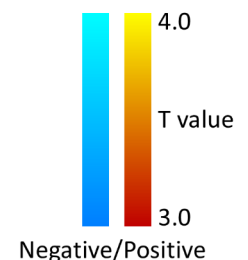
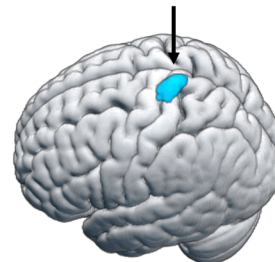


Fig. 4. (A) Left physician-rated rigidity correlated with perfusion positively in the right midbrain and negatively in the right sensory-motor cortex. (B) Right physician-rated rigidity correlated negatively with left sensory-motor cortical perfusion. (C) Left bias difference correlated with perfusion positively in the right substantia nigra and negatively in the right sensory-motor cortex. (D) Right bias difference correlated negatively with left sensory-motor cortical perfusion. No correlation with the elastic coefficient was found on either side. Positive and negative correlations are colored in red-yellow and blue-cyan, respectively. Images were generated using MRICroGL version 1.2 (<https://www.nitrc.org/projects/mricrogl>)³⁷. MNI; Montreal Neurological Institute coordinates.

negatively with left sensory-motor cortex perfusion (Fig. 4D). Both sides of the elastic coefficient did not show significant clusters.

Discussion

This study explored the association between muscle tonus parameters measured by the torque-angle instrument, clinical features, and brain function in PD. The bias difference and the elastic coefficient correlated with the physician-rated rigidity score aligning with previous reports⁵. Notably, the bias difference decreased after dopaminergic medication, whereas the elastic coefficient did not. Higher bias differences were related to lower body mass index, while higher values of the elastic coefficient were related to higher UPDRS total motor scores and PDRP expression. Imaging analysis revealed that the physician-rated rigidity and bias difference correlated positively with right substantia nigra perfusion and negatively with contralateral sensory-motor cortex perfusion.

The torque-angle measuring instrument is feasible for assessing rigidity in PD, potentially compensating for the limitations of video-based motor symptom assessment as it does not require special skills and showed no obvious inter-examiner differences (data not shown). Previous studies using similar techniques, measuring torque-angle during passive flexion and extension, have been reported to evaluate rigidity in the wrist joint in patients with PD^{18–20}. Consistent with the present study, both the bias difference and elastic coefficient showed a linear correlation between muscle tone parameters and physician assessments. Interestingly, they showed discrepant responses to dopaminergic medications in the elastic coefficient^{18–20}. In this study, no statistically significant changes in the elastic coefficient were observed by dopaminergic medication, albeit a relatively larger number of PD patients had participated compared to previous studies. This difference may be attributed to

the sampling bias, as advanced-stage patients were examined in both off and on conditions. Nevertheless, we suggest that the bias difference is a rigidity marker more closely related to physician-rated assessment compared to the elastic coefficient, as it showed a stronger correlation with physician-rated score and a significant change between off and on conditions.

The expression score of SPECT-derived PDRP correlated with the elastic coefficient. Although metabolic PET-derived PDRP is modulated by dopaminergic therapy⁷, the elastic coefficient was constant under both conditions^{7,9,21}. The topography of PDRP identified in this study resembled the FDG PET-derived PDRP⁹ (Fig. 3A). However, a notable discrepancy was observed in the thalamus, showing hypermetabolism in PET-derived PDRP but hypoperfusion in SPECT-derived PDRP. The thalamic activity was observed to be increased in PD compared to healthy subjects, both in glucose metabolism and in cerebral blood flow²². Moreover, dopaminergic agents further increase the regional perfusion in the thalamus in PD^{21,23}. The pattern derived by Tc-^{99m} ethylene cysteinate dimer SPECT showed similar thalamic activity to FDG PET⁸. One explanation for these inconsistencies may be that our PDRP partially reflects PD-related cognitive pattern (PDCP)²¹, which lacks basal ganglia hyperactivity but shows the medial prefrontal and precuneus hypoactivity²¹. Since PDCP is consistent in on and off conditions⁹, it is understandable that the elastic coefficient correlated with SPECT-derived PDRP did not change after dopaminergic medication. In fact, subjects' scores of SPECT-derived PDRP were correlated with those of both PET-derived PDRP and PDCP, which were reported previously²¹ (Supplementary Fig. 2AB). Nevertheless, this SPECT-derived PDRP could be a reliable substitute for PET-derived PDRP because its expression was significantly higher in PD groups compared to healthy controls and correlated with UPDRS part III (Supplementary Fig. 2CD). This study included nine patients with DBS, which can modulate rigidity and PDRP expression^{24,25}. Although the magnitude of the DBS effect may differ between rigidity and PDRP expression, it is significant that the PDRP scores and elasticity coefficients showed a correlation, as both muscle tone and cerebral blood flow were assessed under stimulus-on conditions. Although further validation is needed, the elastic coefficient may be a progression marker independent of dopaminergic therapies in PD.

Furthermore, the bias difference negatively correlated with body mass index, indicating that patients with more severe rigidity tended to have lower weight. Rigidity may be associated with unconscious and unnecessary muscle activity, leading to energy consumption, which could contribute to patient fatigue and weight loss²⁶. Both fatigue and weight loss are known as indicators of poor prognosis in PD, but dopamine replacement therapy may alleviate rigidity, improving fatigue and weight^{27,28}. Therefore, physicians should not overlook rigidity in PD, and a lower bias difference could be considered a treatment goal for preventing weight loss.

The pathophysiological mechanisms of rigidity in PD remain largely unknown. Neurophysiological studies found two aspects of abnormal reactions during passive joint movement in PD patients: exaggerated long-latency stretch reflexes (LLSR) and a combination of enhanced shortening response (SR) and stretch-induced inhibition (SII)⁴. The SR and SII observed in antagonist muscles during passive movement potentially counteract each other, resulting in constant resistance or "lead-pipe" rigidity^{4,29}. Based on the findings that the strength of SR correlated to the elastic coefficient, Xia and colleagues estimated SR and SII separately from the torque-angle graph and concluded both of them contributed to rigidity^{20,29,30}. Some studies suggested that these reactions, characterized by short latency and long duration, should be driven by group II or Ib afferent fibers involving spinal interneurons²⁰. These neurons may be controlled by the brainstem reticular formation, whose hyperactivation may increase muscle tone in PD³¹. The elastic coefficient may be related to overall disease severity and reflect SR and SII since these are peripheral reactions. This is also in line with the result that the elastic coefficient correlated with total UPDRS III and PDRP but was not associated with specific areas of cerebral blood flow.

The bias difference may be associated with another electrophysiological feature of rigidity, LLSR. In the prior studies, the LLSR magnitude correlated with increased muscle tone observed by examiners, whereas SR or SII did not^{32,33}, which aligns with the stronger association between the bias difference and physician-rated rigidity in the current study. LLSR is considered to be a polysynaptic response mediated by cortical and subcortical regions^{4,34}. The primary motor cortex, reticular formation, substantia nigra, and cerebellum are the essential contributors to LLSR³⁴. This aligns with our findings that right substantia nigra perfusion correlated with left bias difference. Higher bias differences were associated with lower perfusion in the contralateral sensory-motor cortex, which was the opposite of what we expected based on the previous knowledge that the primary-motor cortex hyperactivity might be associated with rigidity severity due to the dysfunction of the cortico-basal ganglia-thalamo-cortical motor circuit in PD⁷. Indeed, some evidence suggests increased LLSR largely reflects abnormal activation of a transcortical neural loop involving the sensorimotor cortex^{34,35}, while subcortical white matter regions may be out of scope in this study. On the contrary, neurophysiological studies with non-invasive transcranial magnetic stimulation reported reduced primary motor activity in PD patients³⁶. According to growing experimental data, increased LLSR would be driven by hyperactivity in the pontine reticular formation through the dorsal and medial reticulo-spinal tracts³³. The excitability of stretch reflex circuitry may increase muscle tone, while the circuitry is inhibited by the primary motor cortex through the corticospinal tract, potentially explaining the negative correlation between the bias difference and contralateral sensory-motor cortex perfusion⁴.

Correlation analyses in this study did not focus on the difference between off and on conditions because of the expected increase in beta error resulting from correction for multiple comparisons. In other words, the small number of subjects in this study serves as a limitation in examining such differences. The notable results for the difference are shown in Supplementary Fig. 3. Although there are challenges in reporting statistical significance, a consistent result of the bias difference was observed in both off and on conditions. This suggests that the bias difference serves as an indicator of rigidity, similar to the physician-rated assessment. Further exploration requires a comprehensive investigation with a larger sample size, including PD patients from early to advanced stage. The ambiguity of the test condition is also a weakness of this study. Although the OFF medication condition was defined as the withdrawal of dopaminergic medication for 12 h, most of the patients were taking long-acting drugs such as dopamine agonists and monoamine-B inhibitors. This is a difficult issue to avoid

in clinical research, but it may affect the results. In addition, half of the patients were tested for muscle tone while on medication, although cerebral perfusion was assessed while off medication in all cases. Medication status was included as a covariate in the voxel-based analysis, which may not be sufficient to detect the true relationship between rigidity parameters and regional blood flow. The low resolution of the SPECT image is one of the limitations of this study. The clusters shown were statistically significant but may include other anatomical regions, especially in the case of the brainstem. The substantia nigra hyperperfusion might reflect the activity of other adjacent regions, such as the subthalamic nucleus or red nucleus. Another limitation of this study is the limited coverage of PD biomarkers, such as dopamine transporter imaging.

Conclusions

The bias difference and the elastic coefficient measured by a torque-angle meter are effective quantitative markers of rigidity in PD. The bias difference is closely related to physician-rated assessment and may serve as a treatment marker. Meanwhile, the elastic coefficient may reflect systemic Parkinsonism and disease progression. Finally, the function of the sensory-motor cortex and substantia nigra plays a key role in PD rigidity.

Data availability

The data supporting this study's findings are available from the corresponding author on reasonable request.

Received: 26 November 2024; Accepted: 21 February 2025

Published online: 07 March 2025

References

- Ogawa, M., Oyama, G., Sekimoto, S., Hatano, T. & Hattori, N. Current status of telemedicine for Parkinson's disease in Japan: A Single-Center Cross-Sectional questionnaire survey. *J. Mov. Disord.* **15**, 58–61. <https://doi.org/10.14802/jmd.21096> (2022).
- Ripic, Z. et al. Validity of artificial intelligence-based markerless motion capture system for clinical gait analysis: Spatiotemporal results in healthy adults and adults with Parkinson's disease. *J. Biomech.* **155**, 111645. <https://doi.org/10.1016/j.jbiomech.2023.111645> (2023).
- Espay, A. J. et al. A roadmap for implementation of patient-centered digital outcome measures in Parkinson's disease obtained using mobile health technologies. *Mov. Disord.* **34**, 657–663. <https://doi.org/10.1002/mds.27671> (2019).
- Ganguly, J., Kulshreshtha, D., Almotiri, M. & Jog, M. Muscle tone physiology and abnormalities. *Toxins (Basel)*. **13** <https://doi.org/10.3390/toxins13040282> (2021).
- Endo, T., Okuno, R., Yokoe, M., Akazawa, K. & Sakoda, S. A novel method for systematic analysis of rigidity in Parkinson's disease. *Mov. Disord.* **24**, 2218–2224. <https://doi.org/10.1002/mds.22752> (2009).
- Strafella, A. P. et al. Molecular imaging to track Parkinson's disease and atypical parkinsonisms: new imaging frontiers. *Mov. Disord.* **32**, 181–192. <https://doi.org/10.1002/mds.26907> (2017).
- Perovnik, M., Rus, T., Schindlbeck, K. A. & Eidelberg, D. Functional brain networks in the evaluation of patients with neurodegenerative disorders. *Nat. Rev. Neurol.* **19**, 73–90. <https://doi.org/10.1038/s41582-022-00753-3> (2023).
- Feigin, A. et al. Tc-99m ethylene cysteinate dimer SPECT in the differential diagnosis of parkinsonism. *Mov. Disord.* **17**, 1265–1270. <https://doi.org/10.1002/mds.10270> (2002).
- Hirano, S., Eckert, T., Flanagan, T. & Eidelberg, D. Metabolic networks for assessment of therapy and diagnosis in Parkinson's disease. *Mov. Disord.* **24** (Suppl 2), 725–731. <https://doi.org/10.1002/mds.22541> (2009).
- Vo, A. et al. Parkinson's disease-related network topographies characterized with resting state functional MRI. *Hum. Brain Mapp.* **38**, 617–630. <https://doi.org/10.1002/hbm.23260> (2017).
- Rus, T. et al. Stereotyped relationship between motor and cognitive metabolic networks in Parkinson's disease. *Mov. Disord.* **37**, 2247–2256. <https://doi.org/10.1002/mds.29188> (2022).
- Tang, C. C. et al. Differential diagnosis of parkinsonism: a metabolic imaging study using pattern analysis. *Lancet Neurol.* **9**, 149–158. [https://doi.org/10.1016/s1474-4422\(10\)70002-8](https://doi.org/10.1016/s1474-4422(10)70002-8) (2010).
- Postuma, R. B. et al. MDS clinical diagnostic criteria for Parkinson's disease. *Mov. Disord.* **30**, 1591–1601. <https://doi.org/10.1002/mds.26424> (2015).
- Goetz, C. G. et al. The unified Parkinson's disease rating scale (UPDRS): status and recommendations. *Mov. Disord.* **18**, 738–750. <https://doi.org/10.1002/mds.10473> (2003).
- Tomlinson, C. L. et al. Systematic review of Levodopa dose equivalency reporting in Parkinson's disease. *Mov. Disord.* **25**, 2649–2653. <https://doi.org/10.1002/mds.23429> (2010).
- Cockrell, J. R. & Folstein, M. F. Mini-Mental state examination (MMSE). *Psychopharmacol. Bull.* **24**, 689–692 (1988).
- Spetsieris, P. G. & Eidelberg, D. Scaled subprofile modeling of resting state imaging data in Parkinson's disease: methodological issues. *Neuroimage* **54**, 2899–2914. <https://doi.org/10.1016/j.neuroimage.2010.10.025> (2011).
- Little, S. et al. A torque-based method demonstrates increased rigidity in Parkinson's disease during low-frequency stimulation. *Exp. Brain Res.* **219**, 499–506. <https://doi.org/10.1007/s00221-012-3107-7> (2012).
- van den Noort, J. C. et al. Quantification of hand motor symptoms in Parkinson's disease: A Proof-of-Principle study using inertial and force sensors. *Ann. Biomed. Eng.* **45**, 2423–2436. <https://doi.org/10.1007/s10439-017-1881-x> (2017).
- Xia, R. & Rymer, W. Z. The role of shortening reaction in mediating rigidity in Parkinson's disease. *Exp. Brain Res.* **156**, 524–528. <https://doi.org/10.1007/s00221-004-1919-9> (2004).
- Hirano, S. et al. Dissociation of metabolic and neurovascular responses to Levodopa in the treatment of Parkinson's disease. *J. Neurosci.* **28**, 4201–4209. <https://doi.org/10.1523/jneurosci.0582-08.2008> (2008).
- Peng, S., Eidelberg, D. & Ma, Y. Brain network markers of abnormal cerebral glucose metabolism and blood flow in Parkinson's disease. *Neurosci. Bull.* **30**, 823–837. <https://doi.org/10.1007/s12264-014-1472-x> (2014).
- Jourdain, V. A. et al. Flow-metabolism dissociation in the pathogenesis of levodopa-induced dyskinesia. *JCI Insight.* **1**, e86615. <https://doi.org/10.1172/jci.insight.86615> (2016).
- Shapiro, M. B. et al. Effects of STN DBS on rigidity in Parkinson's disease. *IEEE Trans. Neural Syst. Rehabil. Eng.* **15**, 173–181. <https://doi.org/10.1109/TNSRE.2007.896997> (2007).
- Trost, M. et al. Network modulation by the subthalamic nucleus in the treatment of Parkinson's disease. *Neuroimage* **31**, 301–307. <https://doi.org/10.1016/j.neuroimage.2005.12.024> (2006).
- Markus, H. S., Cox, M. & Tomkins, A. M. Raised resting energy expenditure in Parkinson's disease and its relationship to muscle rigidity. *Clin. Sci. (Lond)*. **83**, 199–204. <https://doi.org/10.1042/cs0830199> (1992).
- Barichella, M., Cereda, E. & Pezzoli, G. Major nutritional issues in the management of Parkinson's disease. *Mov. Disord.* **24**, 1881–1892. <https://doi.org/10.1002/mds.22705> (2009).

28. Capecchi, M. et al. Rest energy expenditure in Parkinson's disease: role of disease progression and dopaminergic therapy. *Parkinsonism Relat. Disord.* **19**, 238–241. <https://doi.org/10.1016/j.parkreldis.2012.10.016> (2013).
29. Xia, R. et al. Differentiation between the contributions of shortening reaction and stretch-induced Inhibition to rigidity in Parkinson's disease. *Exp. Brain Res.* **209**, 609–618. <https://doi.org/10.1007/s00221-011-2594-2> (2011).
30. Xia, R., Muthumani, A., Mao, Z. H. & Powell, D. W. Quantification of neural reflex and muscular intrinsic contributions to parkinsonian rigidity. *Exp. Brain Res.* **234**, 3587–3595. <https://doi.org/10.1007/s00221-016-4755-9> (2016).
31. Delwaide, P. J., Pepin, J. L. & de Maertens, A. Short-latency autogenic Inhibition in patients with parkinsonian rigidity. *Ann. Neurol.* **30**, 83–89. <https://doi.org/10.1002/ana.410300115> (1991).
32. Berardelli, A., Sabra, A. F. & Hallett, M. Physiological mechanisms of rigidity in Parkinson's disease. *J. Neurol. Neurosurg. Psychiatry.* **46**, 45–53. <https://doi.org/10.1136/jnnp.46.1.45> (1983).
33. Asci, F. et al. Rigidity in Parkinson's disease: evidence from Biomechanical and neurophysiological measures. *Brain* **146**, 3705–3718. <https://doi.org/10.1093/brain/awad114> (2023).
34. Kurtzer, I. L. Long-latency reflexes account for limb biomechanics through several supraspinal pathways. *Front. Integr. Neurosci.* **8**, 99. <https://doi.org/10.3389/fnint.2014.00099> (2014).
35. Pruszynski, J. A. et al. Primary motor cortex underlies multi-joint integration for fast feedback control. *Nature* **478**, 387–390. <https://doi.org/10.1038/nature10436> (2011).
36. Suppa, A. et al. The associative brain at work: evidence from paired associative stimulation studies in humans. *Clin. Neurophysiol.* **128**, 2140–2164. <https://doi.org/10.1016/j.clinph.2017.08.003> (2017).
37. Brett, M., Leff, A. P., Rorden, C. & Ashburner, J. Spatial normalization of brain images with focal lesions using cost function masking. *Neuroimage* **14**, 486–500. <https://doi.org/10.1006/nimg.2001.0845> (2001).

Acknowledgements

We greatly appreciate the patients, volunteers, and their families who willingly participated in this study. We also thank the clinical staff in the ward and clinic of the Department of Neurology, Physiological Examination, and Radiology at the Chiba University Hospital. We thank Dr. Hideo Handa for his participation in the Supplementary video. The instrument was produced by Medicalnics. Co., Ltd. (<http://www.medicalnics.co.jp/en/index.html>) and sold and maintained by Fukuda Denshi Co., Ltd. (<https://fukuda.com/>).

Author contributions

Y. Nakano: Conceptualization, Methodology, Software, Validation, Formal analysis, Investigation, Resources, Data Curation, Writing - Original Draft, Visualization, Funding acquisition. S. Hirano: Conceptualization, Methodology, Validation, Formal analysis, Resources, Data Curation, Writing - Original Draft, Visualization, Supervision, Project administration, Funding acquisition. M. Tamura, Y. Koizumi, Y. Kitayama, M. Izumi, M. Suzuki, K. Yamagishi, and Y. Suzuki: Investigation, Resources, Data Curation. S. Ikeda and A. Arase: Investigation, Data Curation. T. Yamamoto, Y. Yamanaka, A. Sugiyama, K. Shibuya, T. Horikoshi, and T. Uno: Resources and Writing - Review & Editing. D. Eidelberg: Validation, Writing - Review & Editing. S. Kuwabara: Conceptualization, Resources, Writing - Review & Editing, Supervision, Project administration.

Declarations

Competing interests

This work was supported by Grant-in-Aid for Scientific Research (KAKENHI) from the Ministry of Education, Culture, Sports, Science and Technology (MEXT) to S.Hirano. (Number 23K06922). Y. Nakano. was awarded Wagner-Torizuka Fellowship 2023–2025 from the Society of Nuclear Medicine and Molecular Imaging (SNMMI), Overseas Research Program 2023 from the Japanese Society of Neurology, and Overseas Research Program 2024 from the Movement Disorders Society of Japan (MDSJ). Other authors declare no conflicts of interest related to this work.

Additional information

Supplementary Information The online version contains supplementary material available at <https://doi.org/10.1038/s41598-025-91567-y>.

Correspondence and requests for materials should be addressed to S.H.

Reprints and permissions information is available at www.nature.com/reprints.

Publisher's note Springer Nature remains neutral with regard to jurisdictional claims in published maps and institutional affiliations.

Open Access This article is licensed under a Creative Commons Attribution-NonCommercial-NoDerivatives 4.0 International License, which permits any non-commercial use, sharing, distribution and reproduction in any medium or format, as long as you give appropriate credit to the original author(s) and the source, provide a link to the Creative Commons licence, and indicate if you modified the licensed material. You do not have permission under this licence to share adapted material derived from this article or parts of it. The images or other third party material in this article are included in the article's Creative Commons licence, unless indicated otherwise in a credit line to the material. If material is not included in the article's Creative Commons licence and your intended use is not permitted by statutory regulation or exceeds the permitted use, you will need to obtain permission directly from the copyright holder. To view a copy of this licence, visit <http://creativecommons.org/licenses/by-nc-nd/4.0/>.

© The Author(s) 2025